CANCER GENOMICS & PROTEOMICS *22*: 496-509 (2025)
doi: 10.21873/cgp.20517

Characterization of the Neoantigen Profile in a Tumor Mutation Burden-high Melanoma Patient With Multiple Metastases

SHUSUKE YOSHIKAWA[1*], CHIE MAEDA[2*], AKIRA IIZUKA[2], TOMOATSU IKEYA[2], KAZUE YAMASHITA[2], TADASHI ASHIZAWA[2], AKARI KANEMATSU[2], HARUO MIYATA[2], YASUFUMI KIKUCHI[2], KENICHI URAKAMI[3], KEIICHI OHSHIMA[4], TAKESHI NAGASHIMA[3,5], KEN YAMAGUCHI[6], YOSHIO KIYOHARA[1] and YASUTO AKIYAMA[2]

[1]Division of Dermatology, Shizuoka Cancer Center Hospital, Shizuoka, Japan;
[2]Immunotherapy Division, Shizuoka Cancer Center Research Institute, Shizuoka, Japan;
[3]Cancer Diagnostic Research Division, Shizuoka Cancer Center Research Institute, Shizuoka, Japan;
[4]Medical Genetics Division, Shizuoka Cancer Center Research Institute, Shizuoka, Japan;
[5]SRL Inc., Tokyo, Japan;
[6]Office of the President Emeritus, Shizuoka Cancer Center, Shizuoka, Japan

Abstract

Background/Aim: Recently, neoantigen (NA) profiling has been intensively performed for the development of novel immunotherapy. We previously reported a melanoma case with a high tumor mutation burden that achieved complete remission after anti-programmed death-1 therapy. We herein revisited the same case, characterized the NA profiles of other metastatic lesions using *in silico* algorithms and *in vitro* CTL assays, and investigated the immunological status, including tumor-infiltrating lymphocytes and the T cell receptor (TCR) repertoire profile, in metastatic sites.
Materials and Methods: NA candidates obtained from whole-exome sequencing were applied to the HLA-binding prediction algorithm, NetMHCpan4.1. HLA-A*2402-restricted sequence candidates with a strong binding capacity (<50 nM) and elution affinity (<1%) were selected and evaluated for synthetic peptide candidates. The immunological status in metastatic sites was characterized using gene expression profiling, immunohistochemistry, and a TCR repertoire analysis.
Results: The genomic analysis revealed that all metastatic sites, such as costal, intra-muscular, and brain lesions, had >1,500 SNVs, and 12 driver mutations were common to all sites. New driver mutations were identified in intra-muscular (KMT2C: p.P3292S) and brain (JAK1: p.S404P) metastases and a functional analysis of these mutations revealed that JAK1 mutation exhibited a promoting effect on invasion activity. CTL assays using synthetic NA peptides identified more NA epitopes in brain metastasis.

continued

[*]These Authors contributed equally to this work.

Yasuto Akiyama, Immunotherapy Division, Shizuoka Cancer Center Research Institute, 1007 Shimonagakubo, Nagaizumi-cho, Sunto-gun, Shizuoka 411-8777, Japan. Tel: +81 559895222 (Ext. 5330), Fax: +81 559896085, e-mail: y.akiyama@scchr.jp

Received December 23, 2024 | Revised January 16, 2025 | Accepted January 31, 2025

Conclusion: These results might suggest that the heterogeneity of driver gene mutations is unremarkable, while immunological response is variable in metastatic sites. As a result, the genomic and immunological investigation has provided a very valuable and informative suggestion regarding better cancer therapy decisions.

Keywords: High TMB melanoma, multiple metastases, neoantigens, driver gene mutations, immunological status.

Introduction

With advances in next-generation sequencing (NGS) technology and RNA sequencing, the identification of novel neoantigens (NA) mainly derived from passenger mutations has been successful in many clinical trials on immune checkpoint blockade therapy (1-3). Specific complex NA-based peptide or mRNA vaccines comprising multiple NA-derived mutant sequences have been developed in early-phase clinical trials for advanced melanoma, non-small cell lung cancers, and pancreatic cancers (4-8). However, the development of efficient NA identification pipelines based on HLA-epitope binding algorithms and HLA-DNA typing tools is still very challenging. Therefore, an HLA-rapid typing tool and high-throughput-based NA identification system are urgently needed (9-11). The NA profiles of multiple metastatic lesions have yet to be elucidated because of immunological editing and heterogeneity inside tumors, which are other challenges that warrant further study.

We previously reported a melanoma case with multiple metastases (rib, intra-muscular and brain) and a high tumor mutation burden (TMB) that achieved complete remission after anti-programmed death-1 (PD-1) therapy. We identified the novel NA ARMT1 in costal metastasis (12). In the present study, we revisited the same case and characterized the immunological features of each metastatic tumor microenvironment using tumor-infiltrating lymphocytes (TIL) and a T cell receptor (TCR) repertoire analysis. We also investigated NA candidate sequences in new metastatic lesions using NGS-based whole-exome sequencing (WES) and HLA-peptide binding algorithms. Consequently, we evaluated the evolutionary landscape of driver gene mutations and characterized the immunological status of multiple metastatic lesions during cancer progression.

Materials and Methods

Reagents and cell lines. Recombinant human (rh) granulocyte macrophage colony-stimulating factor, rh-interleukin (IL)-1β, rhIL-2, rhIL-4, rhIL-7, tumor necrosis factor (TNF)-α, interferon (IFN)-α, IFN-γ, and Poly I/C were used for dendritic cell production and cytotoxic T cell cultures, as previously described (13). TISI cells were used for the IFN-γ production assay. Human melanoma cell lines, such as A357, C32, and RPMI7951 [the American Type Culture Collection (ATCC), Manassas, VA, USA], were used in gene transduction experiments.

The following antibodies were used for immuno-fluorescence (IF) staining. An anti-CD4 mouse monoclonal antibody (4B12, Cat. No. MA5-12259) and anti-CD68 rabbit polyclonal antibody (Cat. No. 25747-1-AP) were purchased from Thermo Fisher Scientific (Waltham, MA, USA). An anti-PD-1 mouse monoclonal antibody (NAT105, Cat. No. ab52587) and anti-FoxP3 mouse monoclonal antibody (236A/E7, Cat. No. ab20034) were purchased from Abcam (Cambridge, UK). An anti-CD8 mouse monoclonal antibody (144B, Cat. No. GTX72053, Gene Tex Inc., Irvine, CA, USA) and anti-CD204 mouse monoclonal antibody (SRA-C6, Cat. No. KT118, Trans Genic Inc., Kobe, Japan) were also purchased.

The HOPE Project at the Shizuoka Cancer Center (SCC). The High-tech Omics-based Patient Evaluation (HOPE) project has been conducted since 2014 according to the Ethical Guidelines for Human Genome and Genetic Analysis Research and this study was approved by the Institutional

Review Board of SCC, Japan (Authorization Number: 25-33). Comprehensive WES with next-generation sequencers and gene expression profiling with DNA microarrays were performed using cancer tissues and PBMCs from cancer patients as previously described (14).

In the present study, we revisited the melanoma case with a high TMB and multiple metastases, investigated NA candidate sequences from new metastatic lesions using NGS-based WES and HLA-peptide binding algorithms, and characterized the immunological status in metastatic sites.

Characterization of immune response-associated gene expression among three metastatic lesions from the high-TMB melanoma patient. The immune response-associated gene panel was previously reported (15). The expression levels of immune response-associated genes were compared among three metastatic lesions from a melanoma patient. Genes with expression levels that changed by more than 10-fold on a log2-transformed scale from those in the costal metastatic lesion were selected.

Peptide synthesis and CTL induction assay. HLA-A*2402-restricted sequence candidates with a strong binding capacity (<50 nM) and elution affinity (<1%) were selected (12 peptide sequences from intra-muscular metastasis and 13 peptide sequences from brain metastasis) and subjected to chemical peptide synthesis in our institute as previously reported.

Regarding peptide-specific CTL induction, cultures of PBMCs from four HLA-A*2402$^+$ cancer patients were used for *in vitro* CTL induction with mature DC stimulations. Briefly, cancer patient-derived CTLs given 2 rounds of a mature DC stimulation were used in the IFN-γ production assay based on a co-culture of CTLs with specific peptide-treated TISI cells.

T cell receptor gene repertoire analysis using human TCRα and TCRβ profiling kit. Total RNAs were isolated from three metastatic tumors (rib, intra-muscular, and brain lesions) and subjected to the Switching Mechanisms at 5' End of RNA Template (SMARTer™) human TCRα and TCRβ profiling kit (Clontech Laboratories Inc., Mountain View, CA, USA) and Miseq NGS system (Illumina Inc., San Diego, CA, USA) as previously reported (15). The TCR repertoire analysis was performed based on hypervariable VDJ segment sequencing using MiTCR software for a T cell receptor sequencing data analysis (http://mitcr.milaboratory.com/).

JAK1 mutant gene transduction into melanoma cell lines. Human melanoma cell lines (A375, C32, and RPMI7951) were subjected to JAK1 mutant (p.S404P) gene transduction. Briefly, *JAK1* mutant (*p*.S404P) gene cDNA was synthesized (Invitrogen, Thermo Fisher Scientific, Waltham, MA, USA), cloned into a vector, and transduced into three melanoma cells using the Neon™ Transfection System via electroporation (Invitrogen). Cells were then seeded at a single-cell level on 96-well microplates using FACSAria (BD Biosciences, Franklin Lakes, NJ, USA). Proliferated clones were selected and JAK1 mutation-harboring clones were screened by Sanger sequencing using a DNA sequencer (3500 xL Genetic Analyzer, Applied Biosystems, Thermo Fisher Scientific). Stable *JAK1* mutant clones were used in invasion assays.

Cell invasion assay. Invasion assays using parental (wild-type *JAK1* gene) and *JAK1* gene mutant melanoma cell lines were performed as previously described (16). Briefly, melanoma cells (2.5×10^4) suspended in serum-free RPMI1640 medium were added to Corning® BioCoat® Matrigel® Invasion Chambers with an 8.0-μm PET Membrane in two 24-well plates (#354480, Corning Inc., Corning, NY, USA) and RPMI1640 medium with 2% FBS was added to the lower wells. After an incubation for 24 h, cells that invaded through the membrane were stained with the Differential Quik III stain kit (Polysciences Inc., Warrington, PA, USA) and counted using microscopy.

Immunofluorescence (IF) staining. Formalin-fixed paraffin-embedded (FFPE) cancer tissue blocks and sections were made from three metastatic tumors derived from a melanoma patient. IF staining was performed using the

Table I. *Genomic characterization of three metastatic lesions from the high-TMB melanoma patient.*

Metastatic site	Costal	Soft tissue (intra-muscular)	Brain (cerebrum)
Histology	Metastatic malignant melanoma	Metastatic malignant melanoma	Metastatic malignant melanoma
GEP data	T and N	T and N	T only
Total SNV#	1542	1730	1739
Frameshift	5	3	8
Missense	1379	1543	1546
Splice	12	14	15
TMB	88	92	91
Candidate peptide	YA001~YA030	YA062~YA073	YA049~YA061

TMB: Tumor mutation burden; SNV: single nucleotide variant.

Opal 4-color IHC kit (Perkin-Elmer Inc., Waltham, MA, USA) and evaluated under a fluorescent Zeiss imager Z1 microscope (Carl Zeiss, Oberkochen, Germany). Positive cell numbers in five fields of view in sections of each tumor at a high magnification (×200) stained with various antibodies were calculated using the image-analyzing software, WinRoof (Mitani Corporation, Tokyo, Japan) based on an in-house algorithm (17).

Statistical analysis. The significance of differences was analyzed using the Student *t*-test, Wilcoxon rank sum test or Mann–Whitney *U*-test. *p*-Values <0.05 were considered to be significant.

Results

Genomic characterization of three metastatic lesions in the high-TMB melanoma patient. Single-nucleotide variants (SNVs) of all exonic mutations in each metastatic tumor included nonsynonymous, synonymous, and indels/frameshift mutations. The methods for assessing TMB were previously described (14). Metastatic sites were costal, intra-muscular, and brain lesions, respectively. Total SNV numbers were similar in the three metastatic sites, and most were missense mutations. The TMB number was approximately 90 in each lesion (Table I).

Time-dependent evolution of genetic mutation profiles in metastatic lesions. Mutant SNVs from various metastatic tumors were classified into driver mutations and passenger mutations (Figure 1). The evolution of genetic mutation profiles in costal, intra-muscular, and brain metastases occurred in a time-dependent manner. Common mutations comprising 1345 SNVs, including 12 driver mutations, were identified in the three metastatic tumors. A new driver mutation (KMT2C: p.P3292S) was confirmed in intra-muscular metastasis, while another new driver mutation (JAK1: p.S404P) was identified in brain metastasis (Figure 1).

Expression levels of core driver gene mutations in three metastatic lesions. Twelve core driver mutations were maintained in every metastatic lesion. In addition, although mutant *PDGFRA* gene expression was upregulated in intra-muscular metastasis, the expression levels of 12 core driver mutations remained unchanged in metastatic lesions (Table II).

Changes in expression levels of immune response-associated genes in three metastatic lesions. Twenty-six genes with expression levels that changed by more than 10-fold on a log2-transformed scale from those in the costal metastatic lesion were selected. Fold changes in gene expression from those in the costal metastatic lesion (rated as 1.0) are shown in Figure 2. In the intra-muscular lesion, the expression of antibody production and tertiary lymphoid structure-associated genes, such as the *CCL19*, *CCL21*, *IL4*, *CXCL13*, and *CD40LIG* genes, was upregulated.

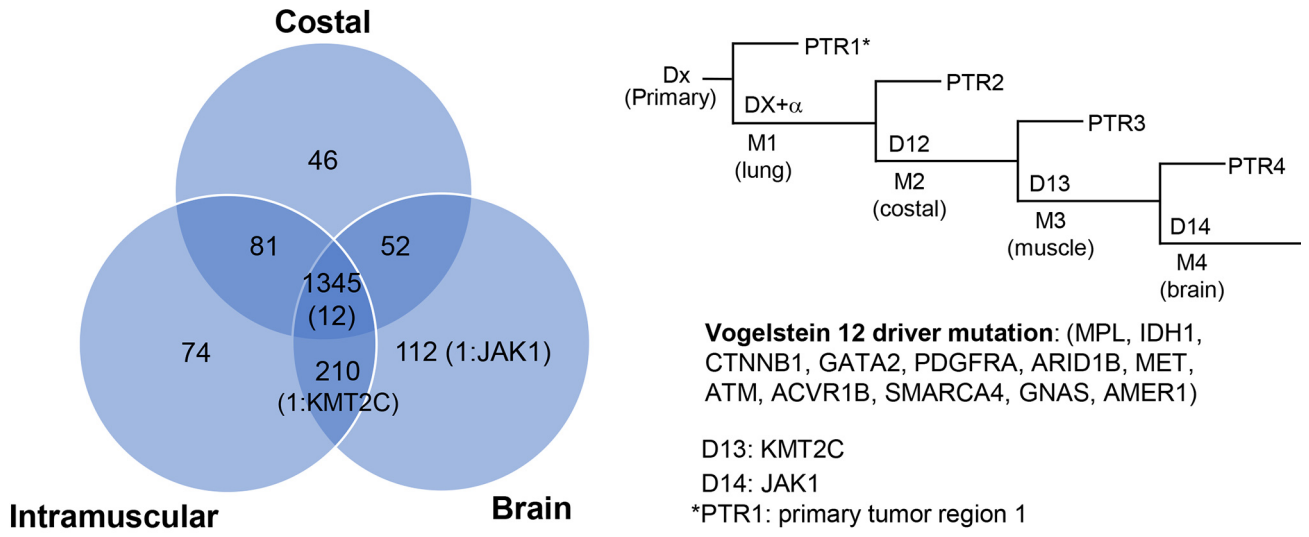

Figure 1. *A genomic analysis of mutational evolution in a metastatic melanoma case. The High-tech Omics-based Patient Evaluation (HOPE) project revealed that all metastatic sites, such as rib, intra-muscular, and brain lesions, had >1,500 SNVs, and 12 driver mutations (MPL, IDH1, CTNNB1, GATA2, PDGFRA, ARID1B, MET, ATM, ACVR1B, SMARCA4, GNAS, and AMER1) were common to all sites. New driver mutations were identified in intra-muscular (KMT2C: p.P3292S) and brain (JAK1: p.S404P) metastases. A functional analysis of these mutations was performed. The phylogenetic tree of mutation evolution in the metastatic melanoma case is shown on the right of the panel. PTR1: Primary tumor region 1.*

Table II. *Expression levels of core driver mutations in various metastatic lesions.*

Gene symbol	Driver mutation	Probe	Normalized values		
			Costal	Intramuscular	Brain
ACVR1B	p.Arg161Ser	A_33_P3364433	−3.60	−3.40	−3.34
AMER1	p.Lys158Ter	A_23_P308150	−1.47	−1.16	−1.68
ARID1B	p.Pro1828His	A_23_P70701	1.23	0.74	0.35
ATM	c.5763-2A>T	A_23_P35916	−1.61	−1.39	−2.41
CTNNB1	p.Pro238Thr	A_23_P29495	4.03	4.46	4.14
GATA2	p.Pro142Gln	A_33_P3550894	−1.88	−1.46	−3.29
GNAS	p.Pro124Leu	A_24_P418809	5.07	4.92	5.97
IDH1	p.Pro147His	A_32_P45009	2.16	2.29	2.78
MET	p.Leu515Phe	A_23_P359245	4.87	5.02	4.36
MPL	p.Arg43Ter	A_24_P156769	−6.30	−5.21	−5.13
PDGFRA	p.His966Tyr	A_23_P300033	−5.88	2.02	−2.07
SMARCA4	p.Pro1180Ser	A_23_P39034	5.25	5.17	4.99
KMT2C	p.Pro3292Ser	A_21_P0011931	1.35	1.45	0.98
JAK1	p.Ser404Pro	A_33_P3784283	−0.56	−0.38	−0.40

The values reflect the gene expression level of core driver gene mutations as indicated in the log2 transformed scale.

In addition, among brain metastasis, the expression of inflammation-associated genes *(TNFRSF11B*, *PTGS2*, and *TREM1*) as well as chemokine genes (CCL3 and CCL4) was upregulated.

Identification of NA candidate peptide sequences and CTL induction activity measurements. Twelve NA peptide candidates (BA <1,000 nM and EL <2% rank) with the HLA-A*2402 restriction were screened from intra-

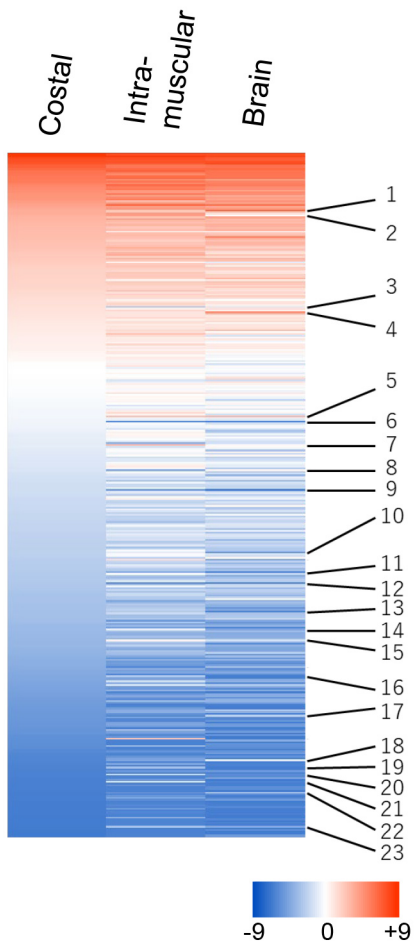

		Fold Change		
		Costal	Intramuscular	Brain
1	CCL3	1.00	0.42	8.37
2	CXCL9	1.00	1.75	0.10
3	CXCL8	1.00	0.07	0.19
4	CCL4	1.00	0.95	14.08
5	TNFRSF21	1.00	10.58	13.50
6	DDX58	1.00	0.02	0.02
7	LRRC32	1.00	14.49	2.16
8	TREM1	1.00	0.13	3.28
9	BMPR1B	1.00	0.10	0.03
10	CXCL13	1.00	2.61	0.10
11	HHLA2	1.00	0.25	0.06
12	HRH4	1.00	0.10	0.07
13	TIGIT	1.00	1.40	0.10
14	CCL19	1.00	6.49	0.53
15	LOXL1	1.00	17.61	4.72
16	TNFSF11	1.00	3.25	0.22
17	PTGS2	1.00	0.61	7.77
18	TNFRSF11B	1.00	3.03	37.71
19	IL4	1.00	9.49	0.81
20	CD40LG	1.00	22.18	1.50
21	CCL21	1.00	37.99	1.15
22	CD21	1.00	1.95	10.15
23	EDA2R	1.00	12.44	4.93

Figure 2. *Changes in expression levels of immune response-associated genes among various metastatic lesions. Twenty-six genes with expression levels showing more than a 10-fold change on a log2-transformed scale in at least one metastatic site from those in the costal metastatic lesion were selected. Actual fold changes in gene expression levels from those in the costal metastatic lesion (rated as 1.0) are shown in the right panel. Red and blue colors in heat map data reflect the relative expression level of the gene, as indicated in the color scale (log2 transformed scale) in the left panel.*

muscular metastasis (SNVs 1543, TMB 92), and only one exhibited significant CTL induction activity in one case of 3 donors (Table III).

Thirteen NA peptide candidates (BA <50 nM and EL <1% rank) with the HLA-A*2402 restriction were identified in brain metastasis (SNVs 1546, TMB 91), and six exhibited significant CTL induction activity in at least one case of 4 donor PBMCs (Table IV). Peptide YA-055 (CLDN10: p.H60Y) exhibited positive CTL induction activity in three cases. These results suggest that SNVs from brain metastasis had more NA peptides with positive CTL induction activity than SNVs from intra-muscular metastasis.

Comparison of TIL profiles in three metastatic lesions. While $CD8^+$ T cell numbers were maintained in every metastatic lesion, the number of $CD8^+PD\text{-}1^+$ T cells slightly increased with the progression of metastasis. $CD4^+Foxp3^+$ regulatory T cell numbers were maintained. Interestingly, the number of immunosuppressive macrophages was significantly higher in brain metastasis than in other metastases (Figure 3).

Table III. *Neoantigen peptide list from intra-muscular metastasis (HLA-A*2402).*

Peptide list	Peptide sequence	Gene name	Mutation	BA model[a] (nM)	EL model[b] (%Rank)	CTL assay
YA-062	ITLFSILRF	ABCC2	N587S	753	0.61	NS
YA-063	CSSTSSFTF	CFAP65	P900S	657	1.3	NS
YA-064	LWGSVLASL	DOPEY2	P193L	397	0.55	NS
YA-065	YYNIDAQTF	GLA	D153N	16.8	0.01	NS
YA-066	TFHLSDLPF	OGDHL	S418F	229	0.37	NS
YA-067	FYMSNIPII	SEC61A1	T286M	10.2	0.04	NS
YA-068	TYPIKLFYM	SEC61A1	T286M	86.4	0.05	NS
YA-069	LYFLETRRL	ST6GAL2	S44Y	302	0.12	NS
YA-070	YMAAAAAAF	TBX3	S615F	200	0.84	NS
YA-071	AWKYTLNNW	TOMM40	G252W	652	0.28	NS
YA-072	MSLAWKYTL	TOMM40	G252W	377	1.1	NS
YA-073	RWYCPRRLL	UNC5CL	H34Y	217	0.48	*p=0.035 (1/3 donors)
CMV-A24	QYDPVAALF	CMVpp65	WT	105	0.01	**p=0.004 (1/3 donors)

[a]BA model: Binding affinity model (NetMHCpan 4.0) for prediction of peptide/HLA affinities. [b]EL model: Eluted ligands model (NetMHCpan 4.1) for prediction of peptide/HLA presentations. IFN-γ production level from neoantigen peptide-stimulated CTLs was compared to that of unstimulated CTLs. Statistically significant; *p<0.05, **p<0.01.

Table IV. *Neoantigen peptide list from brain metastasis (HLA-A*2402).*

Peptide list	Peptide sequence	Gene name	Mutation	BA_model[a] (nM)	EL_model[b] (%Rank)	CTL assay
YA-049	MYFFLSYLF	OR4X1	S65F	7.4	0.04	NS
YA-050	KYLQCPLKF	TRPA1	E668K	16.6	0.01	*p=0.013 (1/4 donors)
YA-051	AYGTLSPTF	PLEKHG5	S826F	18.9	0.01	NS
YA-052	SYSNLHYGF	CAPN13	D182N	20.5	0.01	NS
YA-053	FWPNLCSTF	SLC41A3	P361L	21	0.13	**p=0.002 (1/4 donors)
YA-054	CYITGYAVW	NKAIN2	R60C	21.1	0.11	NS
YA-055	FYCRPHFTI	CLDN10	H60Y	28.1	0.06	**p=0.001 (3/4 donors)
YA-056	LYTPMYLLL	OR2M3	H56Y	31.3	0.01	*p=0.026 (1/4 donors)
YA-057	YFFLSYLFF	OR4X1	S65F	33.1	0.19	NS
YA-058	FYISLGLAF	NIPAL4	G121S	36.8	0.06	**p=0.009 (1/4 donors)
YA-059	IYAFNMNKI	OR6B1	H264Y	37	0.08	NS
YA-060	KYNICVYRW	SLAMF9	Q124K	42.6	0.1	*p=0.01 (1/4 donors)
YA-061	SYLSRHQQI	ZNF347	R617Q	44.3	0.02	NS
CMV-A24	QYDPVAALF	CMVpp65	WT	105	0.01	**p=0.0004 (1/4 donors)

[a]BA_model: Binding affinity model (NetMHCpan 4.0) for prediction of peptide/HLA affinities. [b]EL_model: Eluted ligands model (NetMHCpan 4.1) for prediction of peptide/HLA presentations. IFN-γ production level from neoantigen peptide-stimulated CTLs was compared to that of unstimulated CTLs. Statistically significant; *p<0.05, **p<0.01.

T cell receptor gene repertoire analysis of metastatic melanoma lesions. The results of the T cell repertoire analysis were unremarkable. Although the DE_{50} index was higher in intra-muscular metastasis, no significant changes were observed in the repertoire size or clonal expansion (Figure 4 and Figure 5). The percentage of the top 50 clones was slightly lower in metastatic lesions than in normal tissues.

Effects of JAK1 mutation gene transduction on melanoma cell invasion activity. A *JAK1* mutant gene-transduced RPMI7951 melanoma cell line was successfully obtained

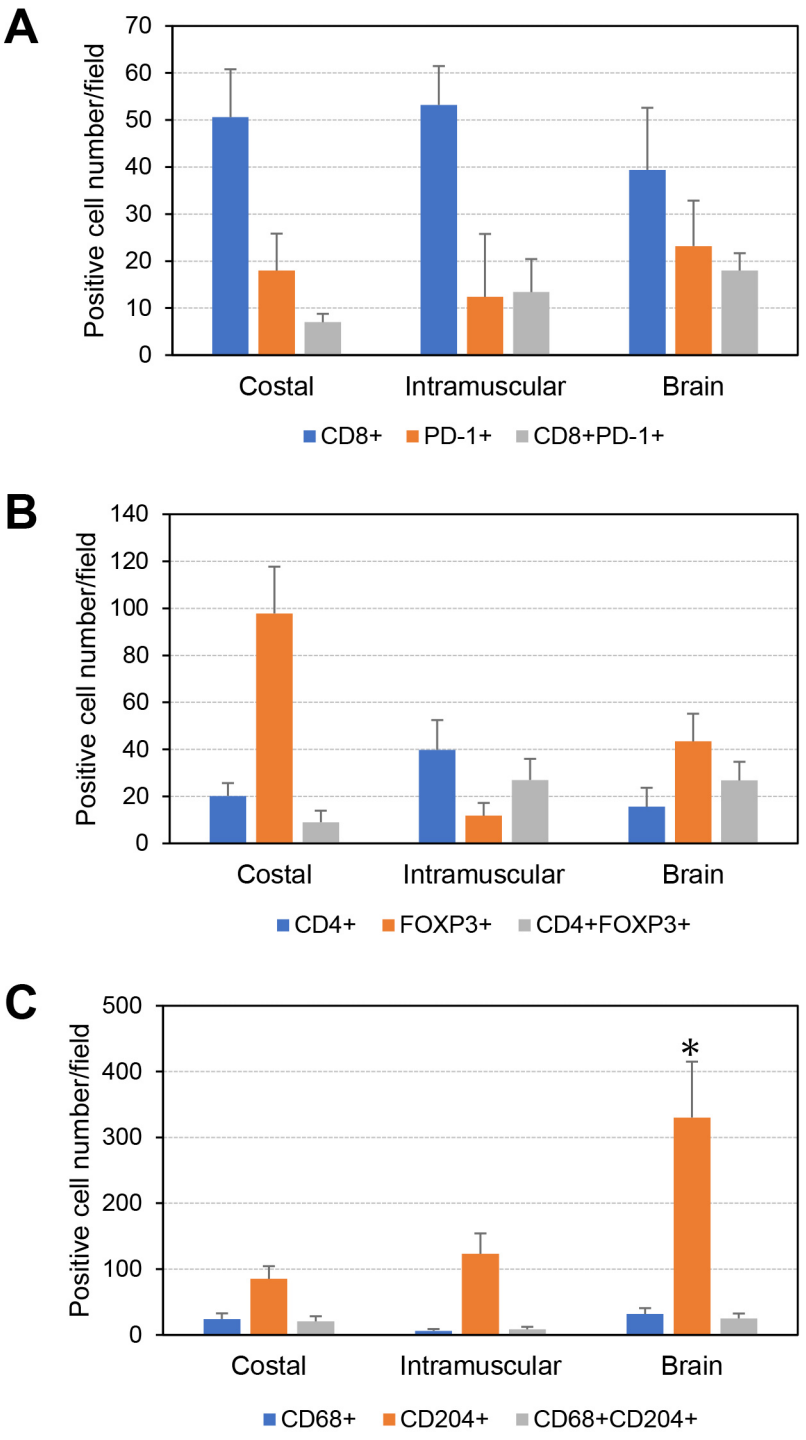

Figure 3. *Comparison of tumor-infiltrating lymphocyte (TIL) profiling among three metastatic lesions. Immunofluorescence staining was performed using the Opal 4-color IHC kit and evaluated under a fluorescent Zeiss imager Z1 microscope. Positive cell numbers in five fields of view in sections of each tumor stained with various antibodies were calculated using the image-analyzing software, WinRoof. Each column shows the mean±standard deviation (SD) of five visual fields. The significance of differences was assessed using the Wilcoxon rank sum test. *p<0.05.*

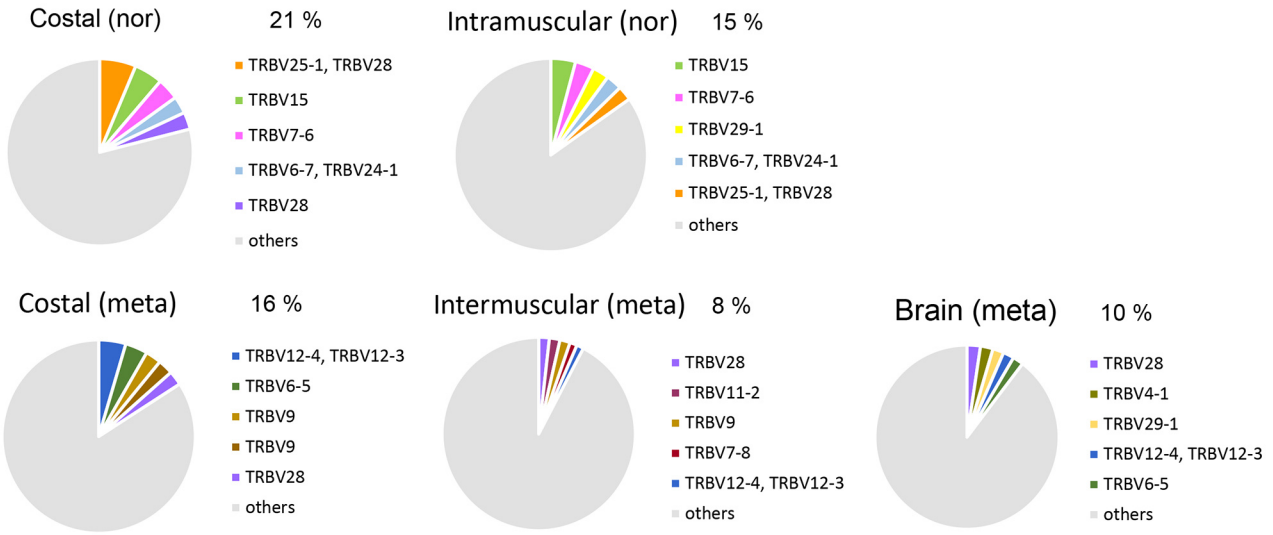

Figure 4. *Comparison of T cell receptor (TCR) gene repertoire clonality among metastatic lesions in a melanoma case. The percentages of the top 50 clones from three metastatic lesions and non-cancerous tissues (normal) are shown. TCR repertoire sequencing data were obtained using a human TCRα and TCRβ profiling kit and the Miseq NGS system. TCR repertoire characterization was performed using the MiXCR software (http://mixcr.milaboratory.com/). TCR: T cell receptor; nor: normal; meta: metastatic.*

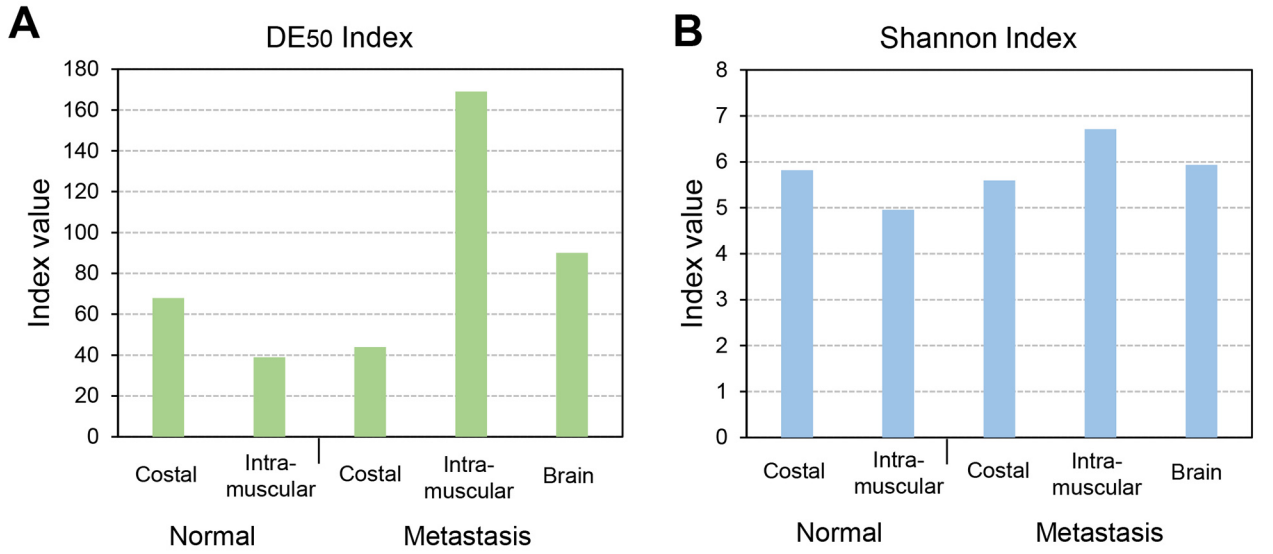

Figure 5. *Comparison of TCR gene repertoire parameters among metastatic lesions in a melanoma case. DE_{50} values (A) and the Shannon index (B) were calculated and compared among three metastatic lesions and non-cancerous (normal)tissues. TCR: T cell receptor.*

using electroporation (Figure 6A). Regarding migration activity without matrigel, no significant difference was noted between vehicle DNA-transduced melanoma cells (control) and *JAK1*-mutant DNA-transduced melanoma cells (mutant) (Figure 6B). On the other hand, *JAK1* mutation-transduced cells exhibited higher invasion activity through matrigel-equipped wells than control cells. In addition, vehicle alone-transduced RPMI7951

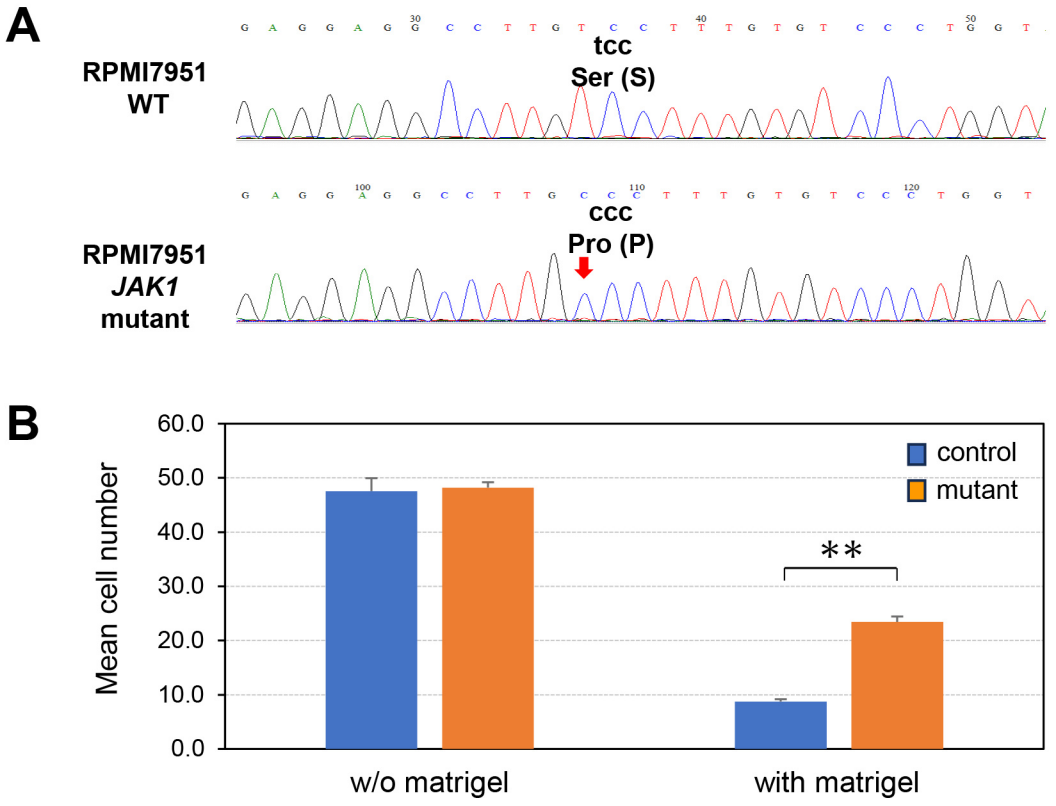

Figure 6. *Effects of JAK1 mutant gene transduction on melanoma cell invasion activity. (A) Successful JAK1 mutant gene transduction confirmed by Sanger sequencing. JAK1 mutant (p.S404P) gene cDNA was synthesized and cloned into the vector. Mutant cDNA was then transduced into RPMI7951 melanoma cells using the Neon™ Transfection System via electroporation, and cells were seeded at a single-cell level. Proliferated clones were selected and JAK1 mutation-harboring clones were screened by Sanger sequencing. (B) The invasion activity of the JAK1 mutant gene-transduced melanoma cell line, RPMI7951. In the invasion assay, cells that invaded through the membrane were stained with the Differential Quik III stain kit and counted using microscopy. The significance of differences was evaluated by the Mann-Whitney U-test. **p<0.01.*

melanoma cells did not show higher invasion activity than parental cells (data not shown).

Discussion

Comprehensive genomic studies using clinical sequencing have enabled us to obtain a substantial amount of multi-omic-based genomic data from various cancer tissues and realize the importance of the evolutional theory to cancer genomics in terms of phylogenetic studies associated with cancer progression and metastasis (18-20).

Genomic analyses using NGS-based WES of cancer metastatic lesions have been performed in many studies in the context of comparisons to primary lesions, and driver mutation signatures are generally considered to be maintained and common through multiple metastatic sites (21-25). On the other hand, previous studies reported genomic heterogeneity, even in the primary tumors, and subclonal heterogeneous cancers may form metastatic sites both spatially and temporally. However, immunological characterization associated with genomic evolutional changes in various metastases has yet to be performed.

We previously reported a melanoma case with multiple metastases and a high TMB, and identified the novel NA ARMT1 in costal metastasis (12). In the present study, we revisited the same case and characterized the

genetic profiles and the immunological status in multiple metastases, including costal, intra-muscular, and brain lesions.

Three metastatic lesions revealed that the minimal driver mutation signature (12 specific driver gene mutations: *MPL*, *IDH1*, *CTNNB1*, *GATA2*, *PDGFRA*, *ARID1B*, *MET*, *ATM*, *ACVR1B*, *SMARCA4*, *GNAS*, and *AMER1*) was maintained with the specific phylogeny of mutation evolution. Priestley *et al*. (23) reported, using whole-genome sequencing data from 2,520 pairs of tumors and normal tissue, that individual metastatic lesions were homogeneous, with the vast majority (96%) of driver mutations being clonal. In addition, Reiter *et al.* (24) analyzed sequencing data for 76 untreated metastases from 20 patients and inferred cancer phylogenies for breast, colorectal, endometrial, gastric, lung, melanoma, pancreatic, and prostate cancers. We found that within individual patients, a large majority of driver gene mutations were common to all metastases.

Intra-tumoral genomic heterogeneity is another important observation in terms of the formation of metastasis based on evolved subclones in other cancer regions (26-28). In the present case, a novel driver mutation was generated in new metastatic lesions; KMT2C: p.P3292S in intra-muscular metastasis and JAK1: p.S404P in brain metastasis. These newly added mutations appeared to be functional because a minimum of 12 driver mutations were still maintained in every metastatic lesion.

We confirmed that that *JAK1* mutation-transduced melanoma cell lines showed higher invasion activity than wild-type parental cells. A total of 112 genetic mutations specific for brain metastasis were recognized; however, possible mutations responsible for brain metastasis have yet to be identified. Only one driver mutation, JAK1: p.S404P was shown to enhance invasion activity, which may be a factor promoting brain metastasis (29-32).

Regarding NA-based CTL epitope identification, the frequency of positive NA peptides exhibiting significant CTL induction activity in any of the volunteer PBMCs was as follows: 1/25 (4%) in rib metastasis previously reported (12), 1/12 (8.3%) in intra-muscular metastasis, and 6/13 (46%) in brain metastasis. The specific mechanisms responsible for the higher frequency of positive CTL production in brain metastasis remain unclear.

The TCR repertoire analysis of metastatic tumor sites did not show significant differences in diversity or clonality, which was not consistent with the higher frequency of positive NA identified in brain metastasis than in other metastatic lesions (33).

We speculate that passenger mutation-based NA were recognized and immunologically edited or deleted through ICB therapy (34-36), and also that common driver mutation-harboring clones were more likely to survive ICB therapy. However, most of these clones, which were sensitive to combination therapy of chemoradiation and surgery, disappeared after an intensive combination treatment. The genomic and immunological investigation of the current metastatic melanoma case has provided a very valuable and informative suggestion regarding better cancer therapy decisions in terms of the combination of ICB with other chemoradiation therapies. In the present melanoma case, all metastatic lesions were successfully treated, and complete remission has been maintained.

Conclusion

These results suggest that the heterogeneity of driver gene mutations is unremarkable, while immunological response is variable in metastatic sites. As a result, the genomic and immunological observations can provide very useful suggestions for better cancer therapy decisions.

Conflicts of Interest

The Authors declare that they have no conflicts of interest.

Authors' Contributions

Conception and study design: SY, CM, and YA. In vitro immunological and other experiments: AI, KY, TA, AK, HM, and YK. Cancer genome sequencing data and gene

expression data analysis: KU, KO, TN, and TI. Manuscript writing: SY, CM and YA. Manuscript review: Yoshio Kiyohara and Ken Yamaguchi. Approval of manuscript: All Authors.

Acknowledgements

We thank the staff of the Shizuoka Cancer Center Hospital for their assistance in sample preparation and the members of the Shizuoka Cancer Center Research Institute for their useful comments.

Funding

This research did not receive any specific grant from funding agencies in the public, commercial, or not-for-profit sectors.

References

1 Nagel R, Pataskar A, Champagne J, Agami R: Boosting antitumor immunity with an expanded neoepitope landscape. Cancer Res 82(20): 3637-3649, 2022. DOI: 10.1158/0008-5472.CAN-22-1525

2 Lybaert L, Lefever S, Fant B, Smits E, De Geest B, Breckpot K, Dirix L, Feldman SA, van Criekinge W, Thielemans K, van der Burg SH, Ott PA, Bogaert C: Challenges in neoantigen-directed therapeutics. Cancer Cell 41(1): 15-40, 2023. DOI: 10.1016/j.ccell.2022.10.013

3 Katsikis PD, Ishii KJ, Schliehe C: Challenges in developing personalized neoantigen cancer vaccines. Nat Rev Immunol 24(3): 213-227, 2024. DOI: 10.1038/s41577-023-00937-y

4 Ott PA, Hu-Lieskovan S, Chmielowski B, Govindan R, Naing A, Bhardwaj N, Margolin K, Awad MM, Hellmann MD, Lin JJ, Friedlander T, Bushway ME, Balogh KN, Sciuto TE, Kohler V, Turnbull SJ, Besada R, Curran RR, Trapp B, Scherer J, Poran A, Harjanto D, Barthelme D, Ting YS, Dong JZ, Ware Y, Huang Y, Huang Z, Wanamaker A, Cleary LD, Moles MA, Manson K, Greshock J, Khondker ZS, Fritsch E, Rooney MS, DeMario M, Gaynor RB, Srinivasan L: A phase Ib trial of personalized neoantigen therapy plus anti-PD-1 in patients with advanced melanoma, non-small cell lung cancer, or bladder cancer. Cell 183(2): 347-362.e24, 2020. DOI: 10.1016/j.cell.2020.08.053

5 Hu Z, Leet DE, Allesøe RL, Oliveira G, Li S, Luoma AM, Liu J, Forman J, Huang T, Iorgulescu JB, Holden R, Sarkizova S, Gohil SH, Redd RA, Sun J, Elagina L, Giobbie-Hurder A, Zhang W, Peter L, Ciantra Z, Rodig S, Olive O, Shetty K, Pyrdol J, Uduman M, Lee PC, Bachireddy P, Buchbinder EI, Yoon CH, Neuberg D, Pentelute BL, Hacohen N, Livak KJ, Shukla SA, Olsen LR, Barouch DH, Wucherpfennig KW, Fritsch EF, Keskin DB, Wu CJ, Ott PA: Personal neoantigen vaccines induce persistent memory T cell responses and epitope spreading in patients with melanoma. Nat Med 27(3): 515-525, 2021. DOI: 10.1038/s41591-020-01206-4

6 Leung CSK, van den Eynde BJ: Combining personalized neoantigen vaccination with chemotherapy and anti-PD-1 to treat NSCLC. Cancer Cell 40(9): 903-905, 2022. DOI: 10.1016/j.ccell.2022.08.002

7 Rojas LA, Sethna Z, Soares KC, Olcese C, Pang N, Patterson E, Lihm J, Ceglia N, Guasp P, Chu A, Yu R, Chandra AK, Waters T, Ruan J, Amisaki M, Zebboudj A, Odgerel Z, Payne G, Derhovanessian E, Müller F, Rhee I, Yadav M, Dobrin A, Sadelain M, Łuksza M, Cohen N, Tang L, Basturk O, Gönen M, Katz S, Do RK, Epstein AS, Momtaz P, Park W, Sugarman R, Varghese AM, Won E, Desai A, Wei AC, D'Angelica MI, Kingham TP, Mellman I, Merghoub T, Wolchok JD, Sahin U, Türeci Ö, Greenbaum BD, Jarnagin WR, Drebin J, O'Reilly EM, Balachandran VP: Personalized RNA neoantigen vaccines stimulate T cells in pancreatic cancer. Nature 618(7963): 144-150, 2023. DOI: 10.1038/s41586-023-06063-y

8 Kamigaki T, Takimoto R, Okada S, Ibe H, Oguma E, Goto S: Personalized dendritic-cell-based vaccines targeting cancer neoantigens. Anticancer Res 44(9): 3713-3724, 2024. DOI: 10.21873/anticanres.17196

9 Yadav M, Jhunjhunwala S, Phung QT, Lupardus P, Tanguay J, Bumbaca S, Franci C, Cheung TK, Fritsche J, Weinschenk T, Modrusan Z, Mellman I, Lill JR, Delamarre L: Predicting immunogenic tumour mutations by combining mass spectrometry and exome sequencing. Nature 515(7528): 572-576, 2014. DOI: 10.1038/nature14001

10 Miller AM, Koşaloğlu-yalçın Z, Westernberg L, Montero L, Bahmanof M, Frentzen A, Lanka M, Logandha Ramamoorthy Premlal A, Seumois G, Greenbaum J, Brightman SE, Soria Zavala K, Thota RR, Naradikian MS, Makani SS, Lippman SM, Sette A, Cohen EEW, Peters B, Schoenberger SP: A functional identification platform reveals frequent, spontaneous neoantigen-specific T cell responses in patients with cancer. Sci Transl Med 16(736): eabj9905, 2024. DOI: 10.1126/scitranslmed.abj9905

11 Gurung HR, Heidersbach AJ, Darwish M, Chan PPF, Li J, Beresini M, Zill OA, Wallace A, Tong AJ, Hascall D, Torres E, Chang A, Lou K', Abdolazimi Y, Hammer C, Xavier-Magalhães A, Marcu A, Vaidya S, Le DD, Akhmetzyanova I, Oh SA, Moore AJ, Uche UN, Laur MB, Notturno RJ, Ebert PJR, Blanchette C, Haley B, Rose CM: Systematic discovery of neoepitope-HLA pairs for neoantigens shared among patients and tumor types. Nat Biotechnol 42(7): 1107-1117, 2024. DOI: 10.1038/s41587-023-01945-y

12 Nonomura C, Otsuka M, Kondou R, Iizuka A, Miyata H, Ashizawa T, Sakura N, Yoshikawa S, Kiyohara Y, Ohshima K, Urakami K, Nagashima T, Ohnami S, Kusuhara M, Mitsuya K, Hayashi N, Nakasu Y, Mochizuki T, Yamaguchi K, Akiyama Y:

Identification of a neoantigen epitope in a melanoma patient with good response to anti-PD-1 antibody therapy. Immunol Lett 208: 52-59, 2019. DOI: 10.1016/j.imlet.2019.02.004

13 Akiyama Y, Oshita C, Kume A, Iizuka A, Miyata H, Komiyama M, Ashizawa T, Yagoto M, Abe Y, Mitsuya K, Watanabe R, Sugino T, Yamaguchi K, Nakasu Y: α-type-1 polarized dendritic cell-based vaccination in recurrent high-grade glioma: a phase I clinical trial. BMC Cancer 12: 623, 2012. DOI: 10.1186/1471-2407-12-623

14 Nagashima T, Yamaguchi K, Urakami K, Shimoda Y, Ohnami S, Ohshima K, Tanabe T, Naruoka A, Kamada F, Serizawa M, Hatakeyama K, Matsumura K, Ohnami S, Maruyama K, Mochizuki T, Kusuhara M, Shiomi A, Ohde Y, Terashima M, Uesaka K, Onitsuka T, Nishimura S, Hirashima Y, Hayashi N, Kiyohara Y, Tsubosa Y, Katagiri H, Niwakawa M, Takahashi K, Kashiwagi H, Nakagawa M, Ishida Y, Sugino T, Takahashi M, Akiyama Y: Japanese version of The Cancer Genome Atlas, JCGA, established using fresh frozen tumors obtained from 5143 cancer patients. Cancer Sci 111(2): 687-699, 2020. DOI: 10.1111/cas.14290

15 Deguchi S, Akiyama Y, Mitsuya K, Ikeya T, Hozumi C, Iizuka A, Miyata H, Maeda C, Ashizawa T, Nagashima T, Urakami K, Ohshima K, Muramatsu K, Sugino T, Ohde Y, Tsubosa Y, Nishimura S, Yamaguchi K: Genetic and immunological characterization of brain metastases from solid cancers. Anticancer Res 44(5): 1983-1994, 2024. DOI: 10.21873/anticanres.17001

16 Akiyama Y, Ashizawa T, Komiyama M, Miyata H, Oshita C, Omiya M, Iizuka A, Kume A, Sugino T, Hayashi N, Mitsuya K, Nakasu Y, Yamaguchi K: YKL-40 downregulation is a key factor to overcome temozolomide resistance in a glioblastoma cell line. Oncol Rep 32(1): 159-166, 2014. DOI: 10.3892/or.2014.3195

17 Miyata H, Akiyama Y, Iizuka A, Kondou R, Maeda C, Kanematsu A, Watanabe K, Ashizawa T, Nagashima T, Urakami K, Ohshima K, Kawata T, Muramatsu K, Shiomi A, Terashima M, Sugino T, Notsu A, Mori K, Yamaguchi K: Development of an automatic measurement method for CD8 and PD-1 positive T cells using image analysis software. Anticancer Res 42(1): 419-427, 2022. DOI: 10.21873/anticanres.15500

18 Schwartz R, Schäffer AA: The evolution of tumour phylogenetics: principles and practice. Nat Rev Genet 18(4): 213-229, 2017. DOI: 10.1038/nrg.2016.170

19 Birkbak NJ, McGranahan N: Cancer genome evolutionary trajectories in metastasis. Cancer Cell 37(1): 8-19, 2020. DOI: 10.1016/j.ccell.2019.12.004

20 Rogiers A, Lobon I, Spain L, Turajlic S: The genetic evolution of metastasis. Cancer Res 82(10): 1849-1857, 2022. DOI: 10.1158/0008-5472.CAN-21-3863

21 Brastianos PK, Carter SL, Santagata S, Cahill DP, Taylor-Weiner A, Jones RT, Van Allen EM, Lawrence MS, Horowitz PM, Cibulskis K, Ligon KL, Tabernero J, Seoane J, Martinez-Saez E, Curry WT, Dunn IF, Paek SH, Park SH, McKenna A, Chevalier A, Rosenberg M, Barker FG 2nd, Gill CM, Van Hummelen P, Thorner AR, Johnson BE, Hoang MP, Choueiri TK, Signoretti S, Sougnez C, Rabin MS, Lin NU, Winer EP, Stemmer-Rachamimov A, Meyerson M, Garraway L, Gabriel S, Lander ES, Beroukhim R, Batchelor TT, Baselga J, Louis DN, Getz G, Hahn WC: Genomic characterization of brain metastases reveals branched evolution and potential therapeutic targets. Cancer Discov 5(11): 1164-1177, 2015. DOI: 10.1158/2159-8290.CD-15-0369

22 De Mattos-Arruda L, Sammut SJ, Ross EM, Bashford-Rogers R, Greenstein E, Markus H, Morganella S, Teng Y, Maruvka Y, Pereira B, Rueda OM, Chin SF, Contente-Cuomo T, Mayor R, Arias A, Ali HR, Cope W, Tiezzi D, Dariush A, Dias Amarante T, Reshef D, Ciriaco N, Martinez-Saez E, Peg V, Ramon Y Cajal S, Cortes J, Vassiliou G, Getz G, Nik-Zainal S, Murtaza M, Friedman N, Markowetz F, Seoane J, Caldas C: The genomic and immune landscapes of lethal metastatic breast cancer. Cell Rep 27(9): 2690-2708.e10, 2019. DOI: 10.1016/j.celrep.2019.04.098

23 Priestley P, Baber J, Lolkema MP, Steeghs N, de Bruijn E, Shale C, Duyvesteyn K, Haidari S, van Hoeck A, Onstenk W, Roepman P, Voda M, Bloemendal HJ, Tjan-Heijnen VCG, van Herpen CML, Labots M, Witteveen PO, Smit EF, Sleijfer S, Voest EE, Cuppen E: Pan-cancer whole-genome analyses of metastatic solid tumours. Nature 575(7781): 210-216, 2019. DOI: 10.1038/s41586-019-1689-y

24 Reiter JG, Makohon-Moore AP, Gerold JM, Heyde A, Attiyeh MA, Kohutek ZA, Tokheim CJ, Brown A, DeBlasio RM, Niyazov J, Zucker A, Karchin R, Kinzler KW, Iacobuzio-Donahue CA, Vogelstein B, Nowak MA: Minimal functional driver gene heterogeneity among untreated metastases. Science 361(6406): 1033-1037, 2018. DOI: 10.1126/science.aat7171

25 Yoshikawa S, Kiyohara Y, Otsuka M, Kondou R, Nonomura C, Miyata H, Iizuka A, Ohshima K, Urakami K, Nagashima T, Kusuhara M, Sugino T, Mochizuki T, Yamaguchi K, Akiyama Y: Multi-omics profiling of patients with melanoma treated with nivolumab in project HOPE. Anticancer Res 37(3): 1321-1328, 2017. DOI: 10.21873/anticanres.11450

26 Gerlinger M, Rowan AJ, Horswell S, Math M, Larkin J, Endesfelder D, Gronroos E, Martinez P, Matthews N, Stewart A, Tarpey P, Varela I, Phillimore B, Begum S, McDonald NQ, Butler A, Jones D, Raine K, Latimer C, Santos CR, Nohadani M, Eklund AC, Spencer-Dene B, Clark G, Pickering L, Stamp G, Gore M, Szallasi Z, Downward J, Futreal PA, Swanton C: Intratumor heterogeneity and branched evolution revealed by multiregion sequencing. N Engl J Med 366(10): 883-892, 2012. DOI: 10.1056/NEJMoa1113205

27 McGranahan N, Swanton C: Clonal heterogeneity and tumor evolution: past, present, and the future. Cell 168(4): 613-628, 2017. DOI: 10.1016/j.cell.2017.01.018

28 Andor N, Graham TA, Jansen M, Xia LC, Aktipis CA, Petritsch C, Ji HP, Maley CC: Pan-cancer analysis of the extent and consequences of intratumor heterogeneity. Nat Med 22(1): 105-113, 2016. DOI: 10.1038/nm.3984

29 Shin DS, Zaretsky JM, Escuin-Ordinas H, Garcia-Diaz A, Hu-Lieskovan S, Kalbasi A, Grasso CS, Hugo W, Sandoval S, Torrejon DY, Palaskas N, Rodriguez GA, Parisi G, Azhdam A, Chmielowski B, Cherry G, Seja E, Berent-Maoz B, Shintaku IP, Le DT, Pardoll DM, Diaz LA Jr, Tumeh PC, Graeber TG, Lo RS, Comin-Anduix B, Ribas A: Primary resistance to PD-1 blockade mediated by JAK1/2 mutations. Cancer Discov 7(2): 188-201, 2017. DOI: 10.1158/2159-8290.CD-16-1223

30 Chen B, Lai J, Dai D, Chen R, Li X, Liao N: JAK1 as a prognostic marker and its correlation with immune infiltrates in breast cancer. Aging (Albany NY) 11(23): 11124-11135, 2019. DOI: 10.18632/aging.102514

31 Albacker LA, Wu J, Smith P, Warmuth M, Stephens PJ, Zhu P, Yu L, Chmielecki J: Loss of function JAK1 mutations occur at high frequency in cancers with microsatellite instability and are suggestive of immune evasion. PLoS One 12(11): e0176181, 2017. DOI: 10.1371/journal.pone.0176181

32 Lin Q, Chen Z, Shi W, Lv Z, Wan X, Gao K: JAK1 inactivation promotes proliferation and migration of endometrial cancer cells via upregulating the hypoxia-inducible factor signaling pathway. Cell Commun Signal 20(1): 177, 2022. DOI: 10.1186/s12964-022-00990-5

33 Kim T, Lim H, Jun S, Park J, Lee D, Lee JH, Lee JY, Bang D: Globally shared TCR repertoires within the tumor-infiltrating lymphocytes of patients with metastatic gynecologic cancer. Sci Rep 13(1): 20485, 2023. DOI: 10.1038/s41598-023-47740-2

34 Angelova M, Mlecnik B, Vasaturo A, Bindea G, Fredriksen T, Lafontaine L, Buttard B, Morgand E, Bruni D, Jouret-Mourin A, Hubert C, Kartheuser A, Humblet Y, Ceccarelli M, Syed N, Marincola FM, Bedognetti D, van den Eynde M, Galon J: Evolution of metastases in space and time under immune selection. Cell 175(3): 751-765.e16, 2018. DOI: 10.1016/j.cell.2018.09.018

35 Nejo T, Matsushita H, Karasaki T, Nomura M, Saito K, Tanaka S, Takayanagi S, Hana T, Takahashi S, Kitagawa Y, Koike T, Kobayashi Y, Nagae G, Yamamoto S, Ueda H, Tatsuno K, Narita Y, Nagane M, Ueki K, Nishikawa R, Aburatani H, Mukasa A, Saito N, Kakimi K: Reduced neoantigen expression revealed by longitudinal multiomics as a possible immune evasion mechanism in glioma. Cancer Immunol Res 7(7): 1148-1161, 2019. DOI: 10.1158/2326-6066.CIR-18-0599

36 Rosenthal R, Cadieux EL, Salgado R, Bakir MA, Moore DA, Hiley CT, Lund T, Tanić M, Reading JL, Joshi K, Henry JY, Ghorani E, Wilson GA, Birkbak NJ, Jamal-Hanjani M, Veeriah S, Szallasi Z, Loi S, Hellmann MD, Feber A, Chain B, Herrero J, Quezada SA, Demeulemeester J, Van Loo P, Beck S, McGranahan N, Swanton C, TRACERx consortium: Neoantigen-directed immune escape in lung cancer evolution. Nature 567(7749): 479-485, 2019. DOI: 10.1038/s41586-019-1032-7